JCE

Journal of Civil Engineering
ISSN 2086 - 1206 E-ISSN 2579 - 9029

Modelling of Reinforced Concrete Coupling Beams with Headed Bars: Verification and Parametric Studies

Joshua F. Krisnajana[a], Asdam Tambusay[b*], Benny Suryanto[c], Priyo Suprobo[b]

Correspondence

[a]Master student in Civil Engineering Department, Institut Teknologi Sepuluh Nopember, ITS Campus, Sukolilo, Surabaya 60111, Indonesia.
[b]Lecturer in Civil Engineering Department, Institut Teknologi Sepuluh Nopember, ITS Campus, Sukolilo, Surabaya 60111, Indonesia.
[c]School of Energy, Geoscience, Infrastructure and Society, Heriot-Watt University, Edinburgh EH14 4AS, Scotland, United Kingdom.

Corresponding author's email address: asdam@its.ac.id

Submitted : 18 July 2023
Revised : 01 September 2023
Accepted : 01 September 2023

Abstract

This paper explores the accuracy of nonlinear finite element procedures implemented in ATENA in predicting the load-deformation response of reinforced concrete coupling beams with headed bars under reversed cyclic loading. In this study, the coupling beam (incorporating headed bars) tested by Seo and co-workers in 2017 is analysed and its response at different lateral drifts is discussed. Parametric analyses, studying the influence of reinforcement layouts, are also presented. It is shown that the hysteresis loops of the coupling beam could be predicted accurately, along with the crack patterns at different stages of loading and failure mode. It is also shown that the omittance of headed bars resulted in more pronounced bond-slip effects and a more severe pinched response in the post-peak region, highlighting the importance of providing adequate headed reinforcement. A similar trend was observed in the coupling beam with the omittance of U-bars and horizontal transverse reinforcements, whereas the reduction of stirrups was found to increase the prominence of shear failure.

Keywords

ATENA, coupling beams, crack pattern, headed bars, hysteresis response, seismic performance.

INTRODUCTION

High-rise construction has increased considerably in recent years due to growing populations and a significant rise in demand for space optimisation in urban areas, including those located in seismic-prone regions. With recent advances in structural design and analysis, as well as innovations in material technology [1-5], it is possible to design high-rise buildings that can withstand extreme loads such as high wind and earthquakes. These advancements have also allowed engineers to come up with increasingly more efficient design and structural systems.

One of the most commonly used lateral force resisting systems for mid- and high-rise construction is coupled shear wall [6-8]. In essence, this system consists of two or more structural walls which are interconnected to each other by relatively short and deep beams (generally referred to as coupling beams). This results in an integral structural wall system with openings between the connecting beams. It is generally known that coupling beams increase the lateral stiffness of a traditional shear wall system and can provide good sources of energy dissipation [9,10]. Regardless of these advantages, however, internal mechanisms and force trajectories created under seismic loading are still less well understood. As a result, more stringent requirements of reinforcement detailing are generally required for coupling beams. This often leads to reinforcement congestion that adds difficulty for implementation on site.

The response of coupling beams with various reinforcement layouts has been the subject of study for several decades. Galano and Vignoli [11] studied the response of 15 short coupling beams under reversed cyclic loading. Four sets of reinforcement layouts were tested, consisting of the following: (a) longitudinal/transverse (conventional) reinforcement; (b) diagonal reinforcement without confining tie bars; (c) diagonal reinforcement with confining tie bars; and (d) rhombic-shape reinforcement. Test results suggested that each beam developed different truss mechanisms after first cracking. Coupling beams reinforced with diagonal and rhombic reinforcement were found to perform better than that reinforced with longitudinal/transverse bars. It was also found that coupling beam with diagonal bars exhibited the highest load capacity amongst the specimens tested, whereas that with rhombic reinforcement exhibited a stable response beyond the post-peak with no shear failure evident.

Fisher and co-workers [12] studied the response of four full-scale coupling beams constructed with high-strength concrete under monotonic loading. They found that the coupling beams with well-detailed stirrups exhibited a load capacity which exceeded the design code maximum limits on shear capacity. Proper detailing was found essential to provide adequate post-peak deformation capacity with gradual degradation of performance. Spalling of side cover concrete could not however be avoided and was found to occur when the coupling beams approached shear failure.

While the response of coupling beams has been studied by various researchers, the majority of the studies have relied on laboratory testing which is limited in many aspects; for instance, in terms of scale of specimens, reinforcement detailing and layout, and test configurations.

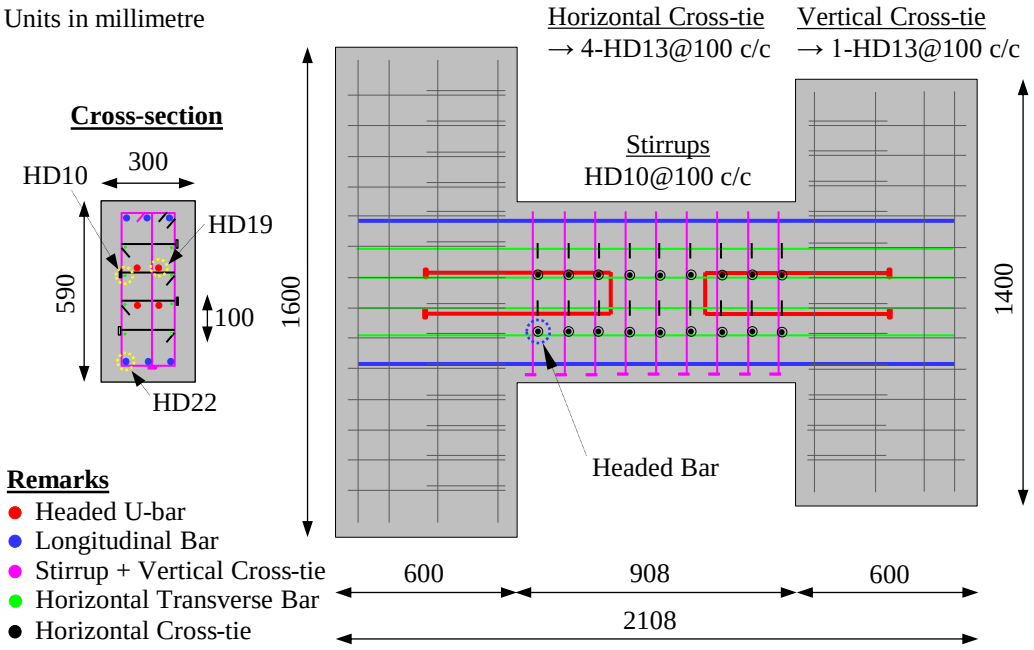

Figure 1 Cross-section details and reinforcement layouts of coupling beam. Adapted from [19].

Table 1 Material properties of concrete and reinforcing bars [19].

Beam	Concrete strength (MPa)	Steel yield strength (MPa)			
		D10	D13	D19	D22
B-2-H	28.7	564	643	543	508

There has been a relatively smaller number of studies focusing on analytical and/or computer simulations; these studies have been mainly undertaken in 2D and involved the use of macro element models [13-15]; the focus of investigations has also been on coupling beams with conventional reinforcement layouts [16-18].

This paper aims to fill the above gaps and provides a guidance into the 3D finite element modelling of reinforced concrete coupling beams. Emphasis is placed on studying the response of a coupling beam with headed bars, which has the potential to address the reinforcement congestion problem. Parametric analyses are also presented to provide insights into the contribution of conventional and headed steel reinforcement and the mechanisms under reversed cyclic loading.

RESEARCH SIGNIFICANCE

Three-dimensional nonlinear finite element tool presented in this article can be used to provide accurate predictions of the response of coupling beams under reversed cyclic loading. Unlike macro models, which can only be used to obtain the hysteresis response, the modelling procedures presented herein can allow for bar detailing and internal mechanisms of resistance to be studied (e.g., stresses and damage in the concrete; bond-slip effects; stresses in the reinforcement; crack patterns and failure mode).

METHODOLOGY

In this section, an overview of the coupling beam specimen, material properties for concrete and reinforcements, as well as finite element model used in this study are described.

A. OVERVIEW OF COUPLING BEAM

The coupling beam specimen referred to in this study was taken from tests carried out by Seo and co-workers in 2017 [19]. Four specimens were tested in total, but only one specimen (B-2-H) was selected and analysed herein. The schematic geometry along with reinforcement detailing are displayed in Figure 1, with relevant details regarding the material properties summarised in Table 1.

As illustrated in Figure 1, the coupling beam was 908mm long, 300mm wide, and 590mm high. It was connected to two rigid concrete blocks with dimensions of 300×600×1600 mm^3 representing shear walls. The coupling beam was reinforced longitudinally with six 22mm headed bars (three placed near the top and bottom faces of the beam) and eight 10mm headed bars (four on each side of the beam at 100mm spacing); four 19mm headed U-bars (two provided at each end of the beam); four 10mm headed horizontal cross-tie at 100mm spacing; and two-legged 10mm closed stirrups at 100mm spacing (each had headed vertical-tie added between the legs). The horizontal and vertical ties had only one headed end (the other end had 135°bent). The headed and bent ends on the horizontal ties were arranged alternately across the beam height, whereas the headed end of the vertical tie was positioned at the bottom face of the beam. For clarity, Figure 1 provides the schematic of all reinforcing bars to allow for better identification of each reinforcement type.

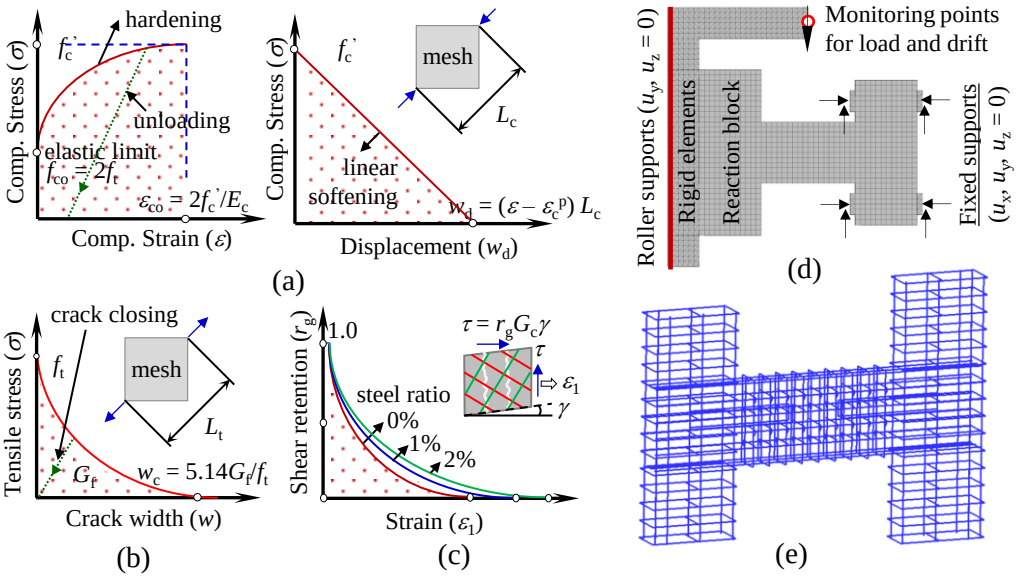

Figure 2. (a) Constitutive models; (b) finite element mesh and boundary conditions; (c) reinforcement layouts.

B. CONSTITUTIVE MODELS

In this paper, the nonlinear finite element analysis software ATENA Science 5.9 [20] was utilised to simulate the response of the coupling beam. Fracture-plastic constitutive models, implemented in the context of smeared fixed crack approach and crush band approach, were employed. Figure 2(a) displays the visual representations of the constitutive models adopted.

The concrete compression model follows the crush band method and Menétrey and Willam plasticity model [21], while the tension model implements the smeared crack approach (adopting the softening model proposed by Hordjik [22]) and utilises the Rankine failure criterion. The shear transfer model considers two main parameters: shear stiffness and shear strength. The shear stiffness is computed based on the shear retention factor proposed by Kolmar [23] whereas the shear strength follows the formulation proposed by Vecchio and Collins [24]. For more detailed information, readers are referred to [25-28].

All reinforcing bars were represented by 2-node truss elements (see Figure 2(c)). The elasto-plastic Menegotto-Pinto model [29] was employed to account for the nonlinear response of steel under cyclic loading. Bond-slip between the headed bar and the concrete follows the formulations in CEB-FIP Model Code 1990 [30].

C. FINITE ELEMENT MODEL

Figure 2(b) displays mesh and boundary conditions used to represent coupling beam B-H-2. Concrete elements were modelled by hexahedral elements with a uniform mesh size of 60 mm, resulting in a total of twelve elements across the depth. Steel plates and rigid components were modelled using tetrahedral elements of the same size and assumed to remain elastic. Full compatibility was enforced at the interface of the two element types.

The shear wall on the right was fixed on four steel plates, with each plate restrained from movement using multiple line supports. Shear wall on the other end was connected to an L-shape rigid frame, which was restrained along the longitudinal direction using roller supports, thereby allowing only lateral movement during loading. The cyclic lateral loads were applied at the end of the rigid frame above the mid-length of the coupling beam, replicating the actual setup and loading protocol adopted in the experiment [19]. Two monitoring points were assigned at the load application point to measure lateral drifts and loads.

RESULTS AND DISCUSSION

A. HYSTERESIS RESPONSE

Figures 3(a) and (b) compare the predicted and observed hysteresis response and backbone curve of coupling beam B-2-H. In general terms, there is a reasonable agreement between the predicted and observed response with regards to the shape of the hysteresis loops, load and drift capacities, unloading and reloading stiffnesses at each loading cycle, as well as the post-peak response in the two loading directions.

Concerning the hysteresis response, it is evident that the predicted response at low drift levels exhibited an accurate representation of the response of the coupling beam under reversed cyclic loading, successfully capturing the strength and stiffness degradation with increasing drift levels up to the peak load. The discrepancy between the predicted and observed peak load was less than 5%, thereby underlining the accuracy of the prediction. As the drift was increased further, the analysis exhibited thicker hysteresis loops with less pinching, but was still capable of capturing the significant strength degradation observed experimentally. The less pinching observed in the post-peak range indicates that the extent of deterioration and/or bond slip of reinforcement in the coupling beam might have been underestimated in the analysis. Nevertheless, it is confirmed that the use of headed bars as a replacement of diagonal bars was found to limit the extent of bond slip of reinforcement up to the peak load which therefore promotes a stable hysteresis response.

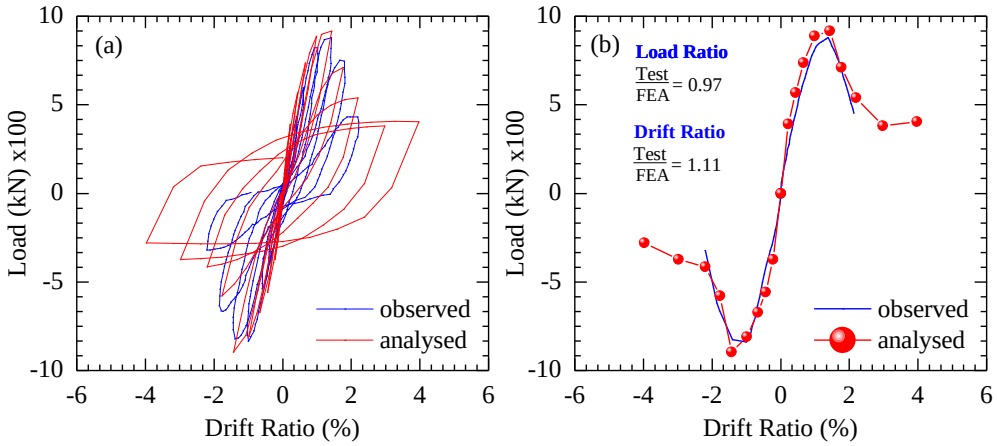

Figure 3 Predicted and observed responses of coupling beam: (a) hysteresis loops and (b) backbone curves.

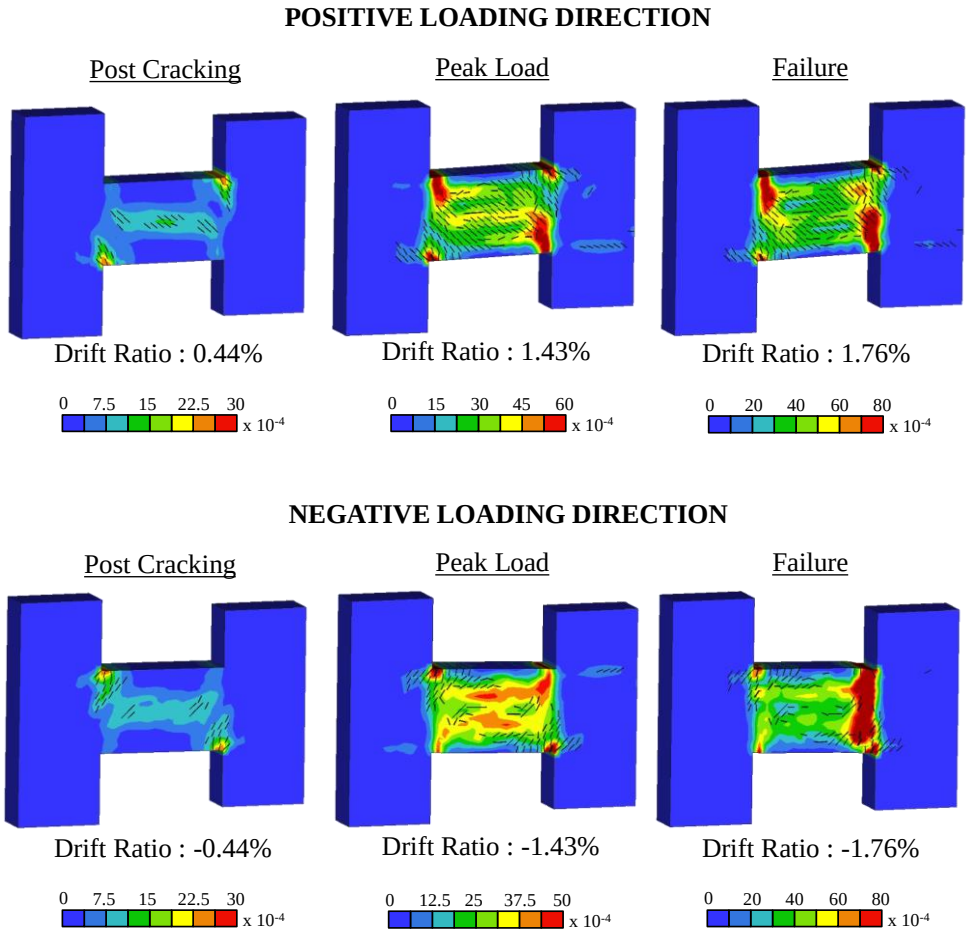

Figure 4 Crack patterns and maximum principal strains of simulated coupling beam B-2-H.

B. CRACK PATTERNS AND FAILURE MODE

To provide insights into the failure mechanisms of the coupling beam at different drift levels, the maximum principal strain obtained from the analysis overlaid with the predicted crack patterns is presented in Figures 4(a)-(c). Three stages of loading were selected which denote the beam conditions after cracking (drift level of 0.44%), peak load (at drift levels of 1.0% and 1.4%) and ultimate load level (at drift levels of 1.4% and 1.8%). The failure crack pattern observed experimentally is also presented in Figure 5 to allow for direct comparison with the results of the analysis.

Concerning the predicted crack pattern at failure, an excellent agreement with the experiment is evident. The extent of damage and the angle of the localised shear crack can be simulated accurately. Cracks are shown to develop initially at the beam-wall interfaces. As the drift increased, new cracks developed diagonally from two opposing

interfaces and spread over the beam span, indicating yielding of reinforcement. As the drift further increased, these pre-existing cracks widened more rapidly and eventually triggered a shear failure at the end.

C. PARAMETRIC STUDY

To provide insights into the influence of reinforcement detailing on the behaviour of the coupling beam, four additional parametric studies were considered which include the following:

(1) The omittance of headed ends (PAR1);
(2) The omittance of U-bars and horizontal transverse bars (PAR2);
(3) Stirrups relaxation with double spacing (PAR3); and
(4) Similar to (2) but with stirrups relaxation (PAR4).

Figures 6(a)-(d) display the schematic of the beam geometry and reinforcement layouts of these four additional beams. The predicted hysteresis responses and crack patterns of the beams are presented in Figures 7(a)-(d).

With reference to Figure 7(a), it is apparent that removing the headed ends was detrimental to the seismic performance of the coupling beam. Not only did the load capacity decrease but also pinching was more pronounced which affected the post-peak response considerably. Regarding Figure 7(b), a similar trend was also observed which therefore suggested that the omittance of U-bars and horizontal transverse bars reduced the load capacity by approximately 24%, but the overall response remained unaltered. The reduction in the number of stirrups (the stirrups spacing doubled) results in a further load reduction (see Figure 7(c)). In addition, it is shown that the increase in stirrups spacing increased the prominence of the localised shear cracks due to a reduction in shear capacity. A similar trend was also observed in Figure 7(d) but with further load capacity reduction due to the combined influence of bar omittance and stirrup relaxation.

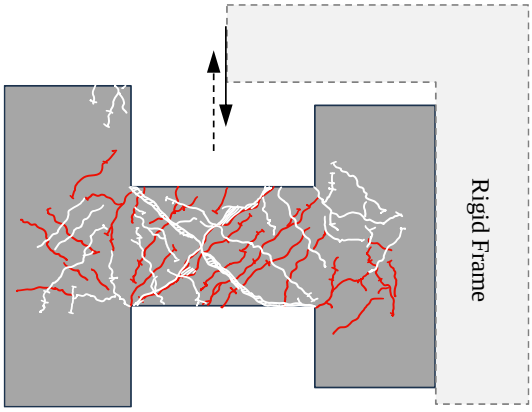

Figure 5 Observed crack pattern. Adapted from [19].

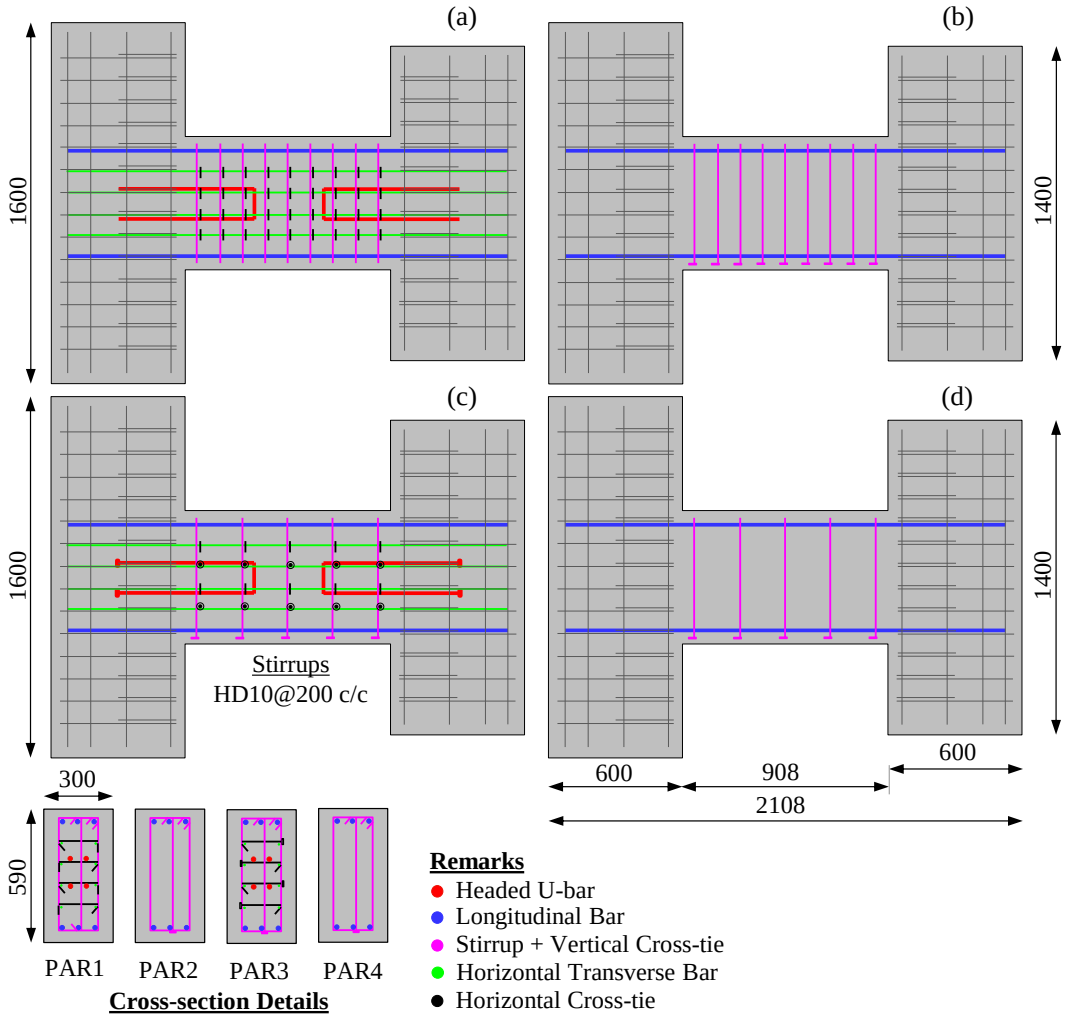

Figure 6 Reinforcement layouts of parametric analyses: (a) PAR1; (b) PAR2; (c) PAR3; and (d) PAR4.

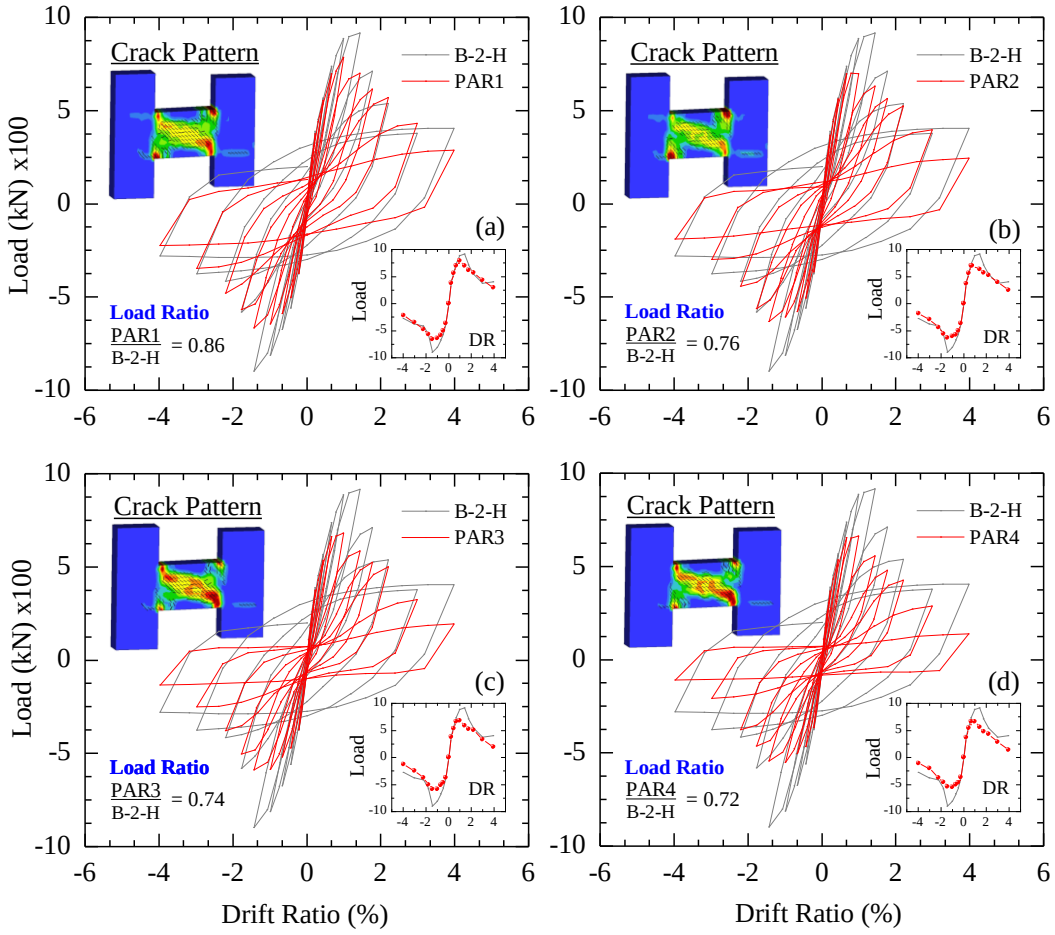

Figure 7 Simulated responses from parametric analyses: (a) PAR1; (b) PAR2; (c) PAR3; and (d) PAR4.

CONCLUSIONS

From the work presented above, the following conclusions are drawn:

1. The constitutive models and modelling procedures adopted in the finite element program ATENA were able to provide accurate predictions of the response of the coupling beam reinforced with headed bars.
2. The predicted hysteresis response was shown to compare well with the observed response, in terms of the load-drift relationships, hysteresis shape, as well as unloading and reloading stiffnesses at each load cycle.
3. Excellent agreement of crack patterns and failure mode with the experimental test was obtained. Failure of the coupling beam was governed by the formation of prominent localised diagonal cracks manifested across the beam span, indicating shear failure.
4. The omittance of headed bars is shown to have detrimental effects on the load capacity due to excessive bond slip of reinforcement at higher loads approaching the peak load. Further omittance of U-bars and horizontal transverse reinforcement was found to yield a similar behavioural response, but with a further reduction in load capacity.
5. A reduction in the amount of stirrups was shown to reduce the overall load capacity and increase the widths of the diagonal cracks.

ACKNOWLEDGEMENT

The authors wish to acknowledge the support of both institutions and for placing the facilities of both institutions at their disposal. This paper was part of a thesis submission by the first author.

REFERENCES

[1] ACI Committee, *ACI-318-19: Building code requirements for structural concrete and commentary*, Farmington Hills: American Concrete Institute, 2019.

[2] Y-C. Lin, R. Sause, J.M. Ricles, "Seismic performance of steel self-centering, moment-resisting frame: hybrid simulations under design basis earthquake," *Journal of Structural Engineering*, vol. 139, no. 11, pp. 1823-1832, 2013.

[3] H. Dabbagh, *Strength and ductility of high-strength concrete shear walls under reversed cyclic loading*, PhD Thesis, The University of New South Wales, Australia, 2005.

[4] A. Tambusay, P. Suprobo, F. Faimun, and A.A. Amiruddin, "Finite element modelling of a reinforced concrete slab-column connection under cyclic load," *International Journal of Applied Engineering Research*, vol. 12, pp. 1987-1993, 2017.

[5] R. Sadjadi, M.R. Kianoush, and S. Talebi, "Seismic performance of reinforced concrete moment resisting

frames," *Engineering Structures*, vol. 29, no. 9, pp. 2365-2380, 2007.

[6] T. Paulay, "Coupling beams of reinforced concrete shear walls," *Journal of the Structural Division*, vol. 97, no. 3, 1971.

[7] N.K. Subedi, "RC-coupled shear wall structures. I: Analysis of coupling beams", *Journal of Structural Engineering*, vol. 117, no. 3, pp. 667-680, 1991.

[8] M-Y. Cheng, R. Fikri, and C-C. Chen, "Experimental study of reinforced concrete and hybrid coupled shear wall systems, *Engineering Structures*, vol. 82, pp. 214-225, 2015.

[9] R. D. Lequesne, G. J. Parra-Montesinos, and J. K. Wight, "Seismic behavior and detailing of high-performance fiber-reinforced concrete coupling beams and coupled wall systems," *Journal of Structural Engineering*, vol. 139, no. 8, pp. 1362–1370, 2013.

[10] N.S. Vu, B. Li, and K. Beyer, "Effective stiffness of reinforced concrete coupling beams," *Engineering Structures*, vol 76, pp. 371-382, 2014.

[11] L. Galano and A. Vignoli, "Seismic behavior of short coupling beams with different reinforcement layouts," *ACI Structural Journal*, vol. 97, no. 6, pp. 876-885, 2000.

[12] A.W. Fisher, E.C. Bentz, and M.P. Collins, "Response of heavily reinforced high-strength concrete coupling beams," *ACI Structural Journal*, vol. 114, no. 6, pp. 1483-1494, 2017.

[13] E. Lim, S-J. Hwang, T-W. Wang, and Y-H. Chang, "An investigation on the seismic behavior of deep reinforced concrete coupling beams," *ACI Structural Journal*, vol. 113, no. 2, pp. 217-226, 2016.

[14] A.E. Toprak, I.E. Bal, and F.G. Gulay, "Review on the macro-modeling alternatives and a proposal for modeling coupling beams in tall buildings," *Bulletin of Earthquake Engineering*, vol. 13, pp. 2309-2326, 2015.

[15] D. Naish, A. Fry, R. Klemencic, and J. Wallace, "Reinforced concrete coupling beams-part II: modeling, *ACI Structural Journal*, vol. 110, no. 6, pp. 1067-1076, 2013b.

[16] H. J. Lee, D. A. Kuchma, W. Baker, and L. C. Novak, "Design and analysis of heavily loaded reinforced concrete link beams for Burj Dubai," *ACI Structural Journal*, vol. 106, no. 3, pp. 383–385, 2009.

[17] E. Lim, S-J. Hwang, C-H. Cheng, and P-Y. Lin, "Cyclic tests of reinforced concrete coupling beam with intermediate span-to-depth ratio, *ACI Structural Journal*, vol. 113, no. 3, pp. 515-524, 2016.

[18] G. Cai, J. Zhao, H. Degee, B. Vandoren, " Shear capacity of steel fibre reinforced concrete coupling beams using conventional reinforcemens, *Engineering Structures*, vol. 128, pp. 428-440, 2016.

[19] S-Y. Seo, H-D. Yun, and Y-S. Chun, "Hysteretic behavior of conventionally reinforced coupling beams in reinforced concrete coupled shear wall," *International Journal of Concrete Structures and Materials*, vol. 11, no. 4, pp. 599-616, 2017.

[20] V. Cervenka, L. Jendele, and J. Cervenka, *ATENA program documentation part 1: theory*, Cervenka Consulting, Prague, 2018.

[21] P. Menetrey and K. J. Willam, "Triaxial failure criterion for concrete and its generalization," *ACI Structural Journal*, vol. 92, no.3, pp. 311-318, 1995.

[22] D.A. Hordijk, *Local approach to fatigue of concrete*, PhD Thesis, Delft University of Technology, 1991.

[23] W. Kolmar, *Beschreibung der kraftuebertragung über risse in nichtlinearen finite-element-berechnungen von stahlbetontragwerken*, PhD Thesis, Darmstadt University of Technology, Germany, 1986.

[24] F. J. Vecchio and M. P. Collins, "The modified compression-field theory for reinforced concrete elements subjected to shear," *ACI Journal*, vol. 83, no.2, pp. 219-231, 1986.

[25] A. Tambusay, P. Suprobo, B. Suryanto, and W. Don, "Application of nonlinear finite element analysis on shear-critical reinforced concrete beams," *Journal of Engineering and Technological Sciences*, vol. 53, no.4, p. 210408, 2021.

[26] W. Don, B. Suryanto, A. Tambusay, and P. Suprobo, "Forensic assessments of the influence of reinforcement detailing in reinforced concrete half-joints: a nonlinear finite element study," *Structures*, vol. 38, pp. 689-703, 2022.

[27] A. Tambusay, B. Suryanto, and P. Suprobo, "Nonlinear finite element analysis of reinforced concrete beam-column joints under reversed cyclic loading," *IOP Conference Series: Materials Science and Engineering*, vol. 930, no.1, p. 012055, 2020.

[28] A. Tambusay, B. Suryanto, P. Suprobo, and J.J.M. Nelson, "Nonlinear analysis of interior and exterior beam-column connections under reversed cyclic loading," *IOP Conference Series: Earth and Environmental Science*, vol. 1195, no.1, p. 012018, 2023.

[29] M. Menegotto and P.E. Pinto, "Method of analysis of cyclically loaded RC plane frames including changes in geometry and non-elastic behavior of elements under combined normal force and bending," *IABSE Symposium*, Lisbon, Portugal, 1973.

[30] CEB-FIP Model Code 1990 Comité Euro-International du Béton Inf. Bullet. pp. 195.